Thermodynamic non-ideality in charge regulation of weak polyelectrolytes

Alejandro Gallegos, Gary M.C. Ong and Jianzhong Wu[1]

Department of Chemical and Environmental Engineering, University of California, Riverside, CA 92521, USA

Supporting Information

1. Change in excess chemical potential upon ionization of a monomer

1) Electrostatic correlation

The electrostatic correlations are accounted by using the mean spherical approximation (MSA)[1].

$$\mu_i^{el} = -l_B\left[\frac{Z_i^2\Gamma}{1+\Gamma\sigma_i}+\eta\sigma_i\left(\frac{2Z_i-\eta\sigma_i^2}{1+\Gamma\sigma_i}+\frac{\eta\sigma_i^2}{3}\right)\right] \quad \text{* MERGEFORMAT (S1)}$$

where $l_B = \beta e^2/4\pi\varepsilon_0\varepsilon_r$ is the Bjerrum length (7.14 Å for water at room temperature), $\beta = 1/k_BT$ is the inverse of the Boltzmann factor, k_B, and the absolute temperature T, e is the elementary charge, and ε_0 and ε_r are the vacuum permittivity and the relative dielectric constant of the solution, respectively, Z_i is the valence of the species, and Γ is the MSA screening parameter which is given by

$$\Gamma^2 = \pi l_B\sum_j \rho_j\left(Z_j^{eff}\right)^2 \quad \text{* MERGEFORMAT (S2)}$$

$$Z_j^{eff} = \frac{Z_j-\eta\sigma_j^2}{1+\Gamma\sigma_j} \quad \text{* MERGEFORMAT (S3)}$$

$$\eta = \frac{1}{H(\Gamma)}\sum_j \rho_j\frac{Z_j\sigma_j}{1+\Gamma\sigma_j} \quad \text{* MERGEFORMAT (S4)}$$

[1]To whom correspondence should be addressed. Email: jwu@engr.ucr.edu

$$H(\Gamma)=\sum_j \rho_j \frac{\sigma_j^3}{1+\Gamma\sigma_j}+\frac{2}{\pi}\left(1-\frac{\pi}{6}\sum_j \rho_j\sigma_j^3\right) \quad \text{* MERGEFORMAT (S5)}$$

2) Charging potential

Because the binding site model requires an analytical expression for the surface potential of the fixed particle, we fit the cDFT predictions of the local electric potential with a DH-like expression over the relevant parameter space ($1\text{Å} < \sigma < 8\text{Å}$ and $c_s < 1$ M):

$$\beta\mu_i^{charge} = Z_i^2 \frac{A_\sigma\sqrt{I}}{1+B_\sigma\sqrt{I}} \quad \text{* MERGEFORMAT (S6)}$$

where A_σ and B_σ are fitting parameters that vary with the diameter of the monomer in angstroms and I is the ionic strength, $I=\sum_j c_j Z_j^2/2$ with c_j being the concentration of species j in the bulk solution. These also will be dependent upon the size of the salt ions present in the solution; however, the sensitivity to the ion size is low at the concentrations considered. The fitting parameters are given by the following equations

$$A_\sigma = 2.27769 + 0.55745\exp\left[-\sigma/2.32949\right] \quad \text{* MERGEFORMAT (S7)}$$

$$B_\sigma = -2.25294 + 2.99137\exp\left[\sigma/25.82945\right] \quad \text{* MERGEFORMAT (S8)}$$

Figure S1a shows the variation of the excess chemical potential with the cesium chloride concentration for a charged hard sphere of diameter 3.57 Å. We see significant changes in both contributions at low salt concentration because they both vary approximately with the square root of the ion concentration. As expected, the increase in salt concentration results in a more negative value, i.e., it shifts the chemical equilibrium towards the ionized state. The combination of these two contributions provides a convenient method to account for the thermodynamic non-ideality in the one-body term.

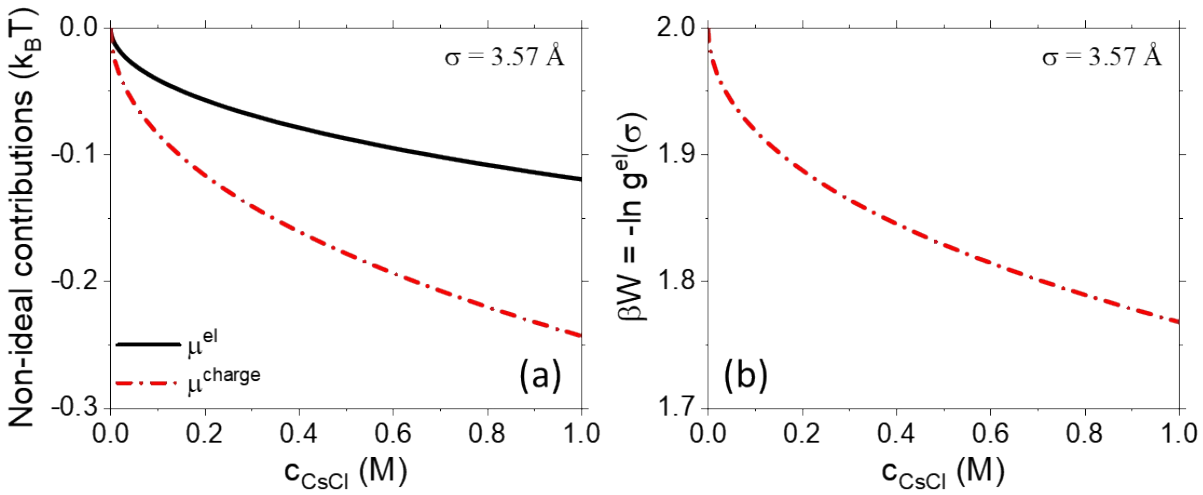

Figure S1. (a) The influence of electrostatic correlations and charging potential on the excess chemical potential for a monomer with a hard-sphere diameter of 3.57 Å. (b) The work to form a bond between two adjacent positive charges at contact from MSA.

2. Site-binding description of poly(acrylic acid)

To demonstrate the power of the nearest-neighbor site-binding model, we consider the titration behavior of poly(acrylic acid), PAA, in a cesium chloride aqueous solution. PAA is a linear chain with low line charge density, i.e., the neighboring sites are not too close, which does not exhibit stereochemistry-dependent titration properties like those of the higher line charge density polyacids.

We show the comparisons of the nearest-neighbor model to the experimental data for poly(acrylic acid) in alkali chloride solutions in Figures S2 and S3[2]. The agreement between the theory and experiments is excellent giving credence to the simplification of the multi-body correlations to that of adjacent monomers at moderate to high salt concentrations.

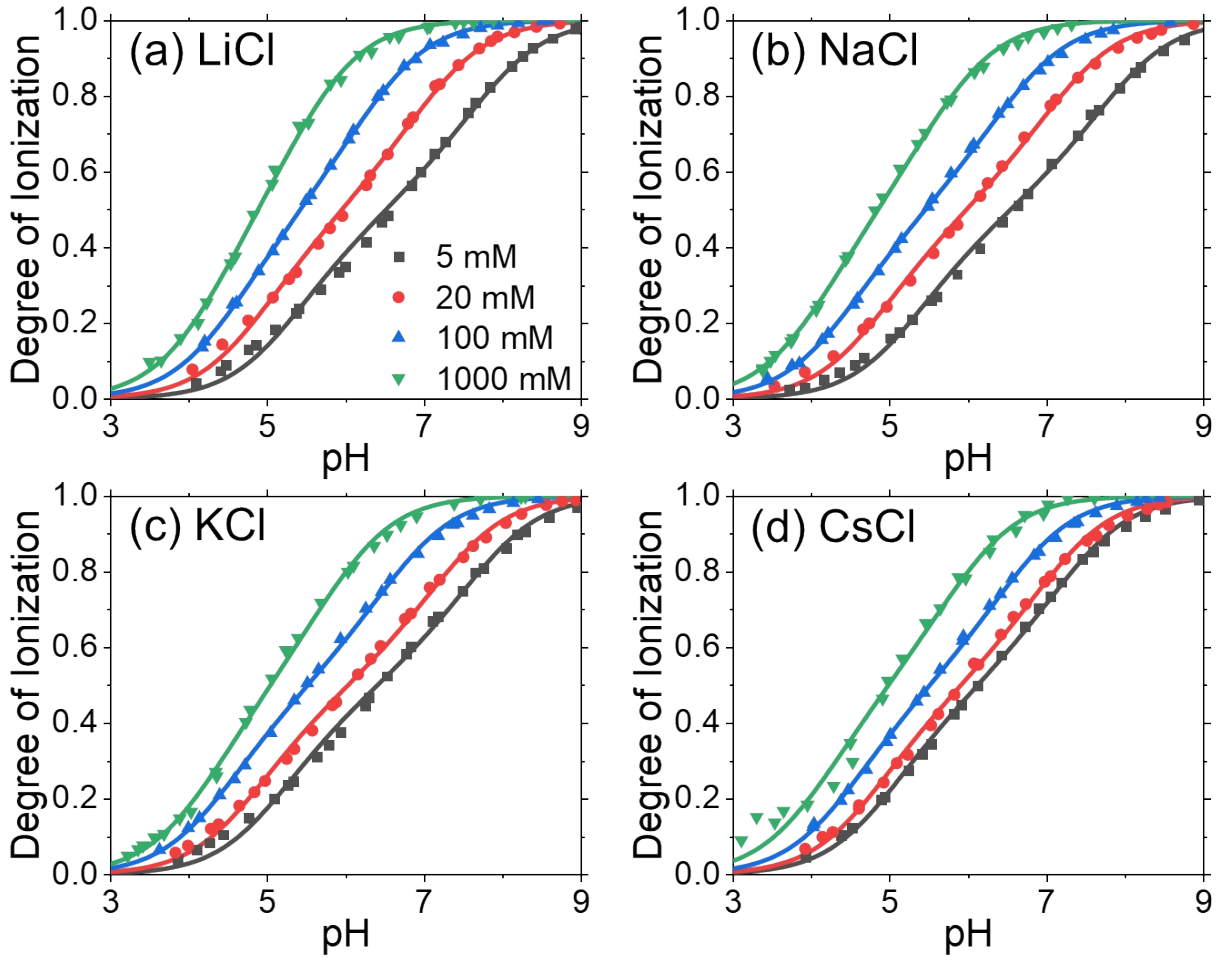

Figure S2. The titration behavior of poly(acrylic acid) in (a) lithium chloride, (b) sodium chloride, (c) potassium chloride and (d) cesium chloride aqueous solution from experiment (symbols) and nearest-neighbor site-binding model (lines).

Figure S3 shows that as the salt concentration is decreased, there is a greater discrepancy between the site-binding model and the experimental results when the polymer is only partially ionized. This can likely be attributed to the long-range interactions not being sufficiently screened. It can be expected that as the ionization of the polymer increases, more counterions will be present in the vicinity of the polymer providing additional screening than compared to the bulk concentration of ions. Such an increase of ions near the polymer has been demonstrated previously

through cylindrical PB calculations[2] and by explicit ion MC simulations[3]. The increased presence of ions near the surface is likely why the nearest-neighbor model is still sufficient even at salt concentrations of 1 mM where it would be expected that interactions beyond the neighboring monomers will be present based on bulk salt concentrations. To compensate, the nearest-neighbor model predicts a larger pK' which misses the initial ionization of PAA. For each solution condition (i.e., salt concentration and cation choice), the apparent dissociation constant and nearest-neighbor pair interaction are determined, and we show these values in Table S1-S4.

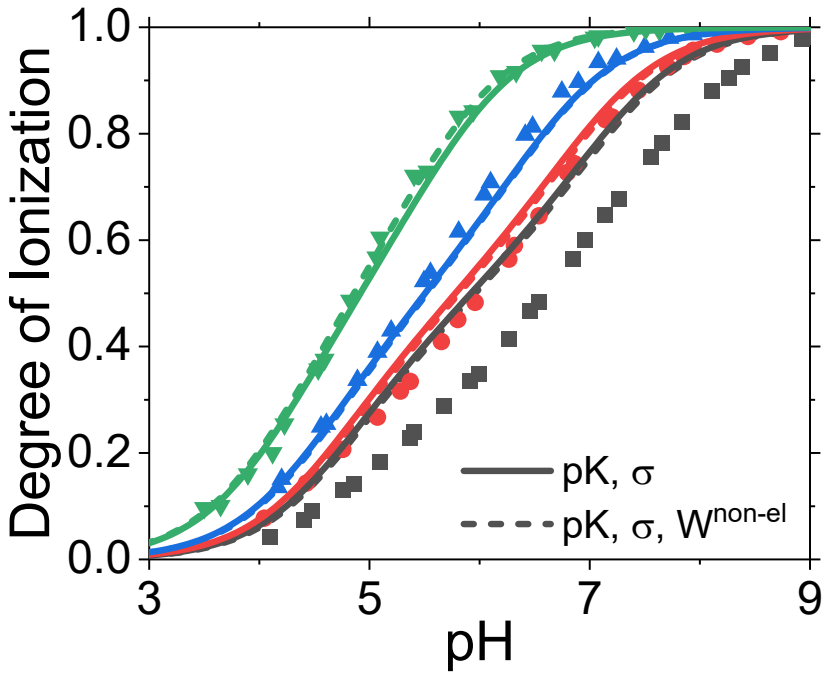

Figure S3. Titration curves for poly(acrylic acid) in aqueous solution of lithium chloride from experiment (symbols) and theoretical correlations (lines). The theoretical lines are fit using the thermodynamic equilibrium constant, size of monomer, and a possible third parameter: the non-electrostatic pair energy.

Based off the fitted parameters, we see that the apparent protonation constant and the nearest-neighbor pair interaction both decrease with increase in salt concentration. This can be understood intuitively as resulting from the electrostatic screening due to the increased number of ions present in the solution. As a result, the ionization (i.e., a decrease in the degree of protonation for a polyacid) increases due to the lower free energy barrier to charge a site. Understandably, at salt concentrations lower than those considered, the importance of interactions beyond nearest neighbor become relevant and the model would not perform well. A major difficulty when employing the nearest neighbor site-binding model is that sufficient experimental data must be available to correlate experimental data and parameters must be determined for every set of solution conditions. Thus, there is no predictive capability to this model which limits its applicability. To improve upon the current approach, we must account for the thermodynamic non-idealities that govern the titration behavior of weak polyelectrolytes.

The titration curve of PAA is only weakly influenced by the incorporation of a non-electrostatic interaction between two consecutive charge sites. However, we find that this leads to an overfitting of the experimental data. The fitting procedure introduces an attractive non-electrostatic energy of -0.59 k_BT to compensate a larger repulsive contribution due to electrostatics for the decreased monomer size (2.73 Å versus 3.56 Å when non-electrostatic interaction was not included). This provides a greater variation with salt concentration which allows a better fit of the 20 mM case. However, the worse agreement of the theoretical results should be attributed to the interactions beyond nearest neighbors. Thus, non-electrostatics are of minor significance to PAA as can be expected from the large separation between sites.

Table S1. The correlated parameters for the nearest-neighbor site-binding model to describe the titration of poly(acrylic acid) in lithium chloride aqueous solution.

c_{LiCl} (mM)	pK'	W^p
5	5.66	1.97
20	5.23	1.67
100	4.85	1.31
1000	4.55	0.78

Table S2. The correlated parameters for the nearest-neighbor site-binding model to describe the titration of poly(acrylic acid) in sodium chloride aqueous solution.

c_{NaCl} (mM)	pK'	W^p
5	5.64	2.07
20	5.18	1.84
100	4.75	1.63
1000	4.37	1.12

Table S3. The correlated parameters for the nearest-neighbor site-binding model to describe the titration of poly(acrylic acid) in potassium chloride aqueous solution.

c_{KCl} (mM)	pK'	W^p
5	5.50	2.08
20	5.16	2.00
100	4.77	1.72
1000	4.53	1.18

Table S4. The correlated parameters for the nearest-neighbor site-binding model to describe the titration of poly(acrylic acid) in cesium chloride aqueous solution.

c_{CsCl} (mM)	pK'	W^p
5	5.33	1.83
20	5.13	1.80
100	4.79	1.65
1000	4.41	1.32

3. Non-electrostatic energy

The inclusion of the non-electrostatic energy is important for differentiating the racemic bond between PMA and PFA as well as the influence of alkali salts on the titration behavior of PMA. If the non-electrostatic pair potential is neglected from the fitting procedure, the distance for the racemic bond is 1.4 Å and for the mesomeric bond is 1.1 Å. This is physically inconsistent since the bond length should be shorter for the racemic bond compared to the mesomeric bond. While the titration curve is similar for PMA with or without the non-electrostatic energy term, this is not the case for PFA (Figure 4S). The reason is the substantial difference in the repulsion between two charged sites connected by a mesomeric bond (+6.5 k_BT vs. +3.7 k_BT when non-electrostatic energy was included). This impacts the PFA titration more since PFA is dominated by mesomeric bonds.

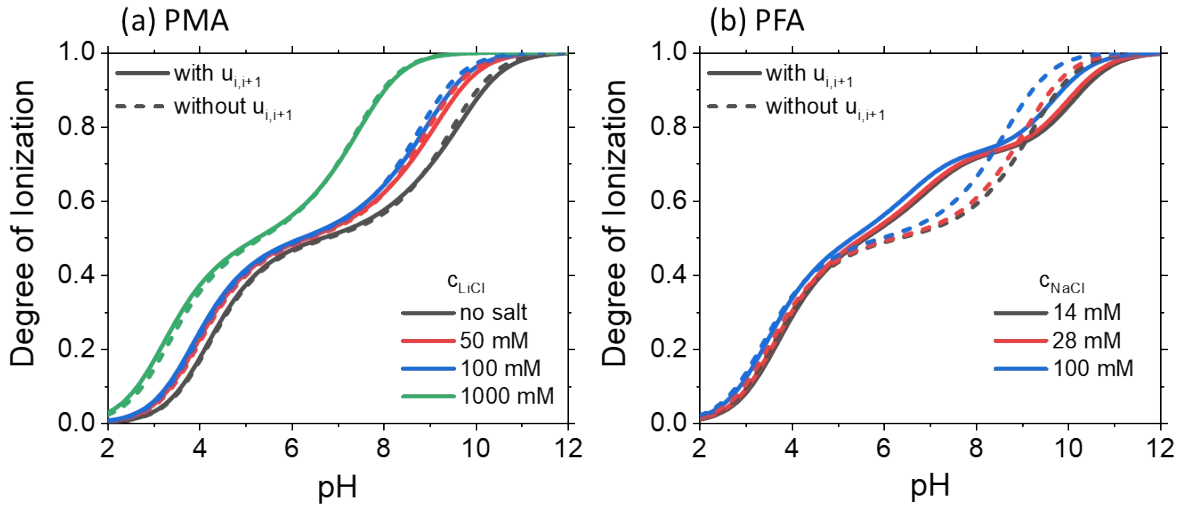

Figure S4. The degree of ionization for (a) poly(maleic acid) in pure water and in three lithium chloride solutions and (b) poly(fumaric acid) in three sodium chloride solutions according to theory (lines) with and without the non-electrostatic energy pair potential included in the fitting procedure.

4. Additional results for dendrimers (see main text for more explanations)

Figure S5 compares the theoretical results with 1 and 2 equilibrium constants for a dendrimer case. When the equilibrium constant is fixed at pK_{out} (i.e., the equilibrium constant for a generation 1 dendrimer), we see noticeably deviations between the theoretical prediction of the titration curve and experiment.

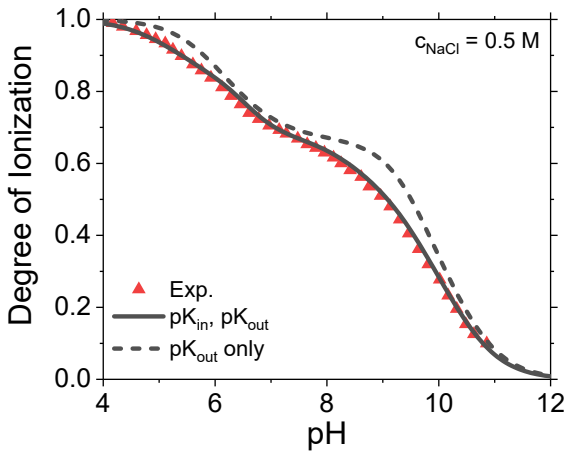

Figure S5. The titration curves for 1,4-diaminobutane poly(propylene imine) (PPI) dendrimer of generation 5 in aqueous solutions at 0.5 M sodium chloride according to experiments[4] (symbols) and theory (lines). The theoretical prediction uses either one or two equilibrium constants to describe the ionization behavior.

Figure S6 illustrates how branching affects the titration curves if one a single equilibrium constant is used. In general, the titration remains similar until the dendrimer has two-thirds of its sites ionized. Beyond this point, further ionization becomes more difficult as the number of dendrimer generation increases.

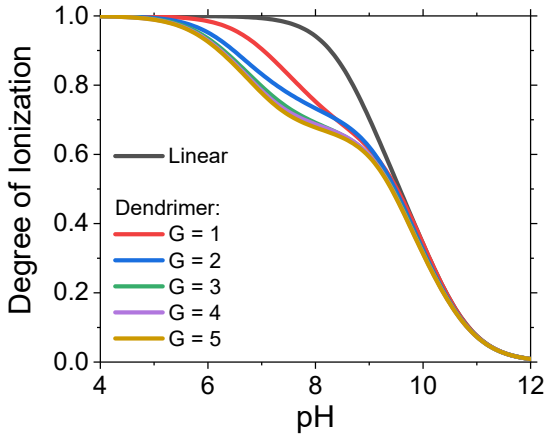

Figure S6. Influence of architecture on the ionization behavior of basic polymers. The equilibrium constant is fixed to $pK_{out} = 9.37$ and $\sigma_t = 4.21\text{Å}$.

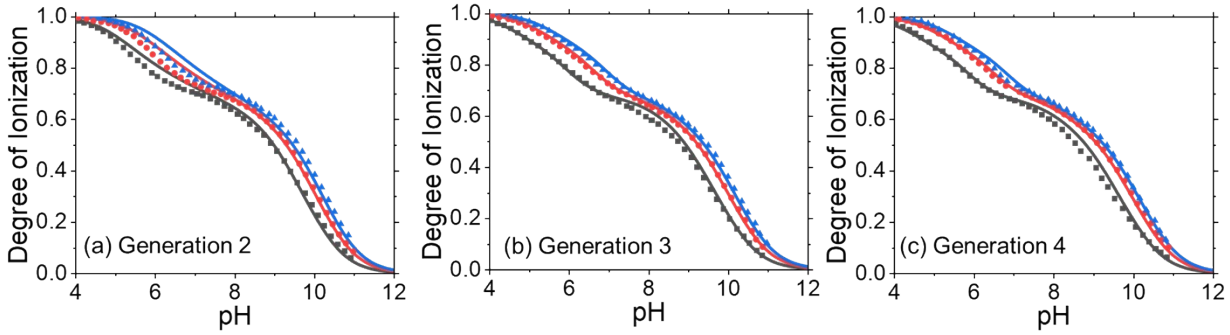

Figure S7. The titration curves for 1,4-diaminobutane poly(propylene imine) (PPI) dendrimers in aqueous solutions at three concentrations of sodium chloride according to experiments[4] (symbols) and theory (lines).

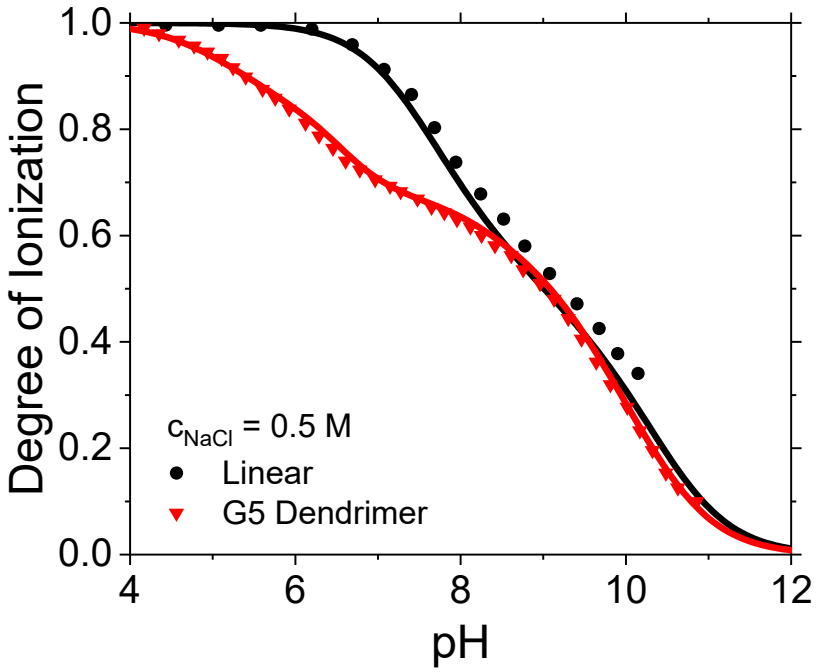

Figure S8. The titration curves of a linear PPI and a generation 5 PPI dendrimer at 0.5 M sodium chloride concentration from experiments (symbols)[4, 5] and theoretical prediction (lines).

Lastly, we consider the prediction for a linear PPI at 0.5 M sodium chloride concentration. For the linear PPI, we use the parameters determined previously for the dendrimer case (viz. $\sigma = 4.21\text{Å}$, $\text{pK} = 9.37$, and $\beta u_{i,i+1} = 1.68$). As shown in Figure S8, our model is able to capture the ionization of both the linear and branched polymers with the same set of parameters. In comparison with our model, the experimental data indicate that the linear polymer ionizes at a slightly higher pH with a smaller rate of charge accumulation when the pH falls. To account for this trend, we need a slightly larger pK value, i.e., a high reversible work to charge adjacent ionizable sites. The discrepancy reflects the differences in the chemical environment of a monomer in the linear versus branched architectures. It may also be attributed to the differences in the hydration energy of ionizable sites because those in the linear chain is smaller than the dendrimer case.

References:

1. L. Blum, *Molecular Physics*, 1975, **30**, 1529-1535.
2. A. Sadeghpour, A. Vaccaro, S. Rentsch and M. Borkovec, *Polymer*, 2009, **50**, 3950-3954.
3. V. S. Rathee, H. Sidky, B. J. Sikora and J. K. Whitmer, *Polymers*, 2019, **11**, 183.
4. R. C. van Duijvenbode, M. Borkovec and G. J. M. Koper, *Polymer*, 1998, **39**, 2657-2664.
5. M. Borkovec and G. J. Koper, 2013.